ultrasonograms made by glass plate (*1*) or digital technique became light-opaque at high information densities (*2*) (Fig. 2).

Although acoustic holographic systems in theory produce a three-dimensional image, in practice it is possible to observe only a single plane at a time in the focal zone. In addition, the quality of the image produced by acoustic holography is poorer than that produced by pulse echo systems. The higher acoustic energies used by these instruments is also undesirable (*3*).

For these reasons, optical holographic reconstruction of pulse echo ultrasonograms was chosen over acoustic holography for three-dimensional ultrasonography.

Ultrasound mammography is carried out by serially sectioning the breast in a vertical direction at 3-mm intervals (Fig. 3). Figure 4 illustrates the preparation of an optical hologram of the three-dimensional ultrasonogram. Ultrasonogram A is placed in position A on Fig. 4, and the film is placed at plane A′. An optical hologram of ultrasonogram A is taken. Ultrasonogram B is now placed in position B and the same film is moved to plane B′. A second optical hologram of ultrasonogram B is recorded on the same film, thus producing a superimposition optical hologram of Fig. 4, A and B. In a similar fashion, ultrasonogram C is placed in position C and the same film is moved to plane C′. By this method the superimposition hologram shown in Fig. 5 has been prepared (*4*).

When the resulting optical hologram is viewed with a laser light beam, a three-dimensional image of the organ is observed. Figure 5 illustrates the ability of the optical hologram to cause a cyst to stand out, with simultaneous display of the fine breast structure. Since this is a flat photograph, the observer loses the three-dimensional effect which is present when the hologram is viewed under laser light. Further improvements in the ultrasonic images may also be obtained by optical deblurring and data processing of ultrasound mammograms prior to the formation of an optical hologram.

The methods outlined are applicable to the study of all organs that can be serially scanned and represent a unique way of studying organs in three dimensions. For ultrasound mammography in particular, it holds the promise of improved detection, localization, and differential diagnosis because this mode of display facilitates interpretation by making it possible to trace the course of ducts, blood vessels, fascial planes, and muscles.

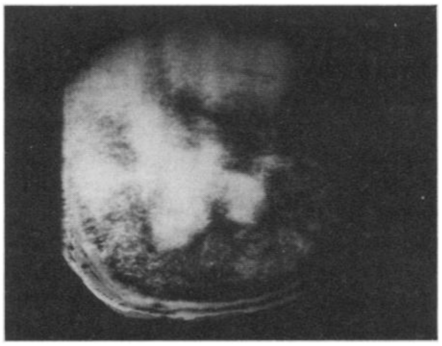

Fig. 5. The internal structure of the breast is visualized in three dimensions when the optical hologram is viewed in laser light. The optical hologram causes the cyst within this breast to stand out. The fine structures of the breast are simultaneously displayed.

In summary, optical holographic reconstruction has been used to form three-dimensional ultrasonograms. This technique has been applied to ultrasound mammography. Its use reduces the volume of ultrasonic data and permits the visualization of organ structure in three dimensions without superimposition and shadowing. This major advance in ultrasonic imagery may make practical the application of pulse echo techniques for cancer detection surveys.

GILBERT BAUM
Department of Ophthalmology,
Albert Einstein College of Medicine,
Bronx, New York 10461
GEORGE W. STROKE
Departments of Electrical Sciences and
Medical Biophysics, State University of
New York, Stony Brook 11794

References and Notes

1. G. Baum and I. Greenwood, *N.Y. State J. Med.* **61**, 4149 (1961).
2. D. E. Robinson, *J. Acoust. Soc. Am.* **52**, 673 (1972).
3. B. Brenden, "Liquid surface ultrasonic holography in interaction of ultrasound and biological tissues" (Publication FDA 73-8008 BRH/DHEW 73-1, Department of Health, Education, and Welfare, Rockville, Md., 1973).
4. G. W. Stroke, *An Introduction to Coherent Optics and Holography* (Academic Press, New York, ed. 2, 1969).
5. The ultrasonograms used in this report and in the preparation of the hologram were produced under contract NO1-CB-23872 of the National Breast Cancer Task Force of the National Cancer Institute. We thank L. Beiser of the Gabor Laboratory, CBS Laboratories, Stamford, Conn., for preparing the hologram.

17 December 1975; revised 7 May 1975

Biological Uptake of Dissolved Silica in the Amazon River Estuary

Abstract. *Approximately 25 percent of the dissolved silica carried by the Amazon River is depleted through diatom production in the inner estuary. Annual production of opaline frustules is estimated to be 15 million tons. However, few diatoms accumulate in modern shelf sediments and chemical recycling appears to be slight. Instead, many frustules apparently are transported landward into the river system, where they deposit in dunes and layers on and within mud and sand bars.*

Rivers contain approximately two orders of magnitude more dissolved silica than does surface ocean water. The fact that this transition from silica-rich to silica-poor water often takes place abruptly in coastal estuaries is most easily explained by conservative dilution of river effluent by ocean water (*1–3*). Uptake of silica by clay minerals may be important in the global chemical budget (*4*), but evidence for chemical removal in estuaries is lacking (*5*). Biological uptake of silica has not been confirmed in any major estuary (*6*), although opaline diatoms often are common in estuarine waters. For instance, diatom populations in the brackish surface waters off the Amazon River exceed 1 to 4 mg/liter (*7*), a sufficiently large quantity to affect the silica concentration. The significance of this process can be appreciated when one considers that the Amazon contributes approximately 40 percent of the dissolved silica brought into the Atlantic Ocean (*8*).

During a recent cruise of the R.V. *Chain* (10 to 18 June 1974) we studied further the possible interactions between diatom production and uptake of dissolved silica in the Amazon estuary. Samples for salinity, suspended matter, dissolved silica, and other chemical parameters were taken at closely spaced intervals while the ship was carrying out geophysical studies in the area; additional samples were collected at four hydrographic stations and from the tops of two gravity cores. In total, more than 120 suspended matter and 60 silica samples were taken (Fig. 1) and analyzed (*9*).

The Amazonian rainy season (February through June) was unusually wet in 1974, and during the period of observation winds were unusually low (often less than 3 m/sec). As a result, the Amazon River effluent (defined by the 10 per mil isohaline) extended more than 200 km offshore (Fig. 1). Because of the lack of mixing, however, the freshwater lens was very thin, and on the inner shelf near-bottom salinities (at 5 to 7 m) ranged from 14 to 19 per mil.

Surface waters near the mouth of the river contained more than 140 mg of suspended matter per liter, mostly terrigenous grains. Seaward, however, concentrations decreased markedly, even though salinities increased only slightly; at 0.5 per mil terrigenous suspensions averaged 20 mg/liter, and at 1.5 per mil concentrations were less than 8 mg/liter (Fig. 2B). Between salinities of 1.5 and 4.0 per mil terrigenous content remained relatively constant, but it decreased sharply as salinity increased further. At 6 per mil the surface waters contained less than 0.5 mg of terrigenous grains per liter, and at 10 per mil concentrations were less than 0.05 mg/liter (Fig. 2B). This two-step decrease in terrigenous grain concentration could indicate two distinct types of deposition (*10*), one caused by the decrease in vertical turbulence as the river widens onto the shelf and the other by flocculation or agglomeration of clay particles (*11*).

Combustible particulate organic matter decreased gradually with increasing salinity and constituted the major component across most of the shelf (Fig. 2B). Diatom frustules were uncommon in the river water, but increased markedly at about 3 per mil (probably in response to increased clarity of surface waters due to deposition of terrigenous grains) and exceeded 2 mg/liter at about 5 per mil; the dominant species was *Coscinodiscus lineatus*. Diatom populations decreased at higher salinities, although they remained the dominant noncombustible suspended component (*12*) (Fig. 2B).

The marked increase in diatom concentration in surface waters was reflected by the decrease in dissolved silica. Between salinities of 0 and 3 per mil, silica concentration followed a predicted dilution curve, while most silica values in surface waters with salinities greater than 8 per mil followed a lower dilution curve (Fig. 2A). In contrast to observations from other estuaries, these two linear dilution curves are separated by a gap of approximately 30 μmole/liter, undoubtedly related to silica uptake by the production of diatom frustules. Assuming that opaline frustules contain 60 percent SiO_2, 30 μmole of SiO_2 would produce 3 mg of diatom frustules per liter, which agrees closely with our observations of suspended matter.

The utilization of 30 μmole of SiO_2 per liter would amount to an annual production of more than 15 million tons of diatomaceous sediment within the Amazon estuary. However, little of this material appears to be preserved within shelf sediments, even though low rates of modern sedimentation on the Amazon shelf (*13*) should preclude the masking of diatoms by terrigenous grains. Our data indicate no recycling of the frustules within the water column. Many silica concentrations in the subsurface waters follow the river-ocean dilution curve, while others coincide with the lower curve in Fig. 2A. The higher values most likely represent subsurface mixing of Amazon River water and ocean water; the absence of silica uptake in these subsurface waters is reasonable since the low level of light penetration would severely restrict the production of phytoplankton (*14*). Diatoms that do reach the bottom may dissolve at or near the sediment-water interface, as SiO_2 concentrations in these waters are significantly enriched (Fig. 2A); however, silica released from clay mineral diagenesis also could cause such values.

Therefore, most frustules must be trans-

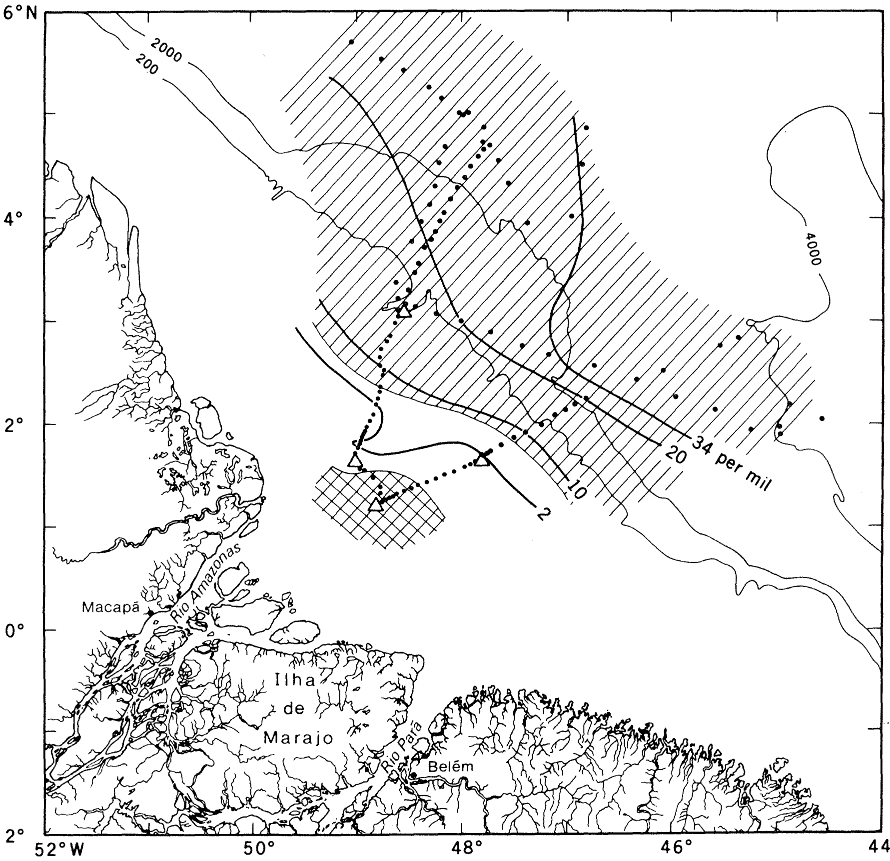

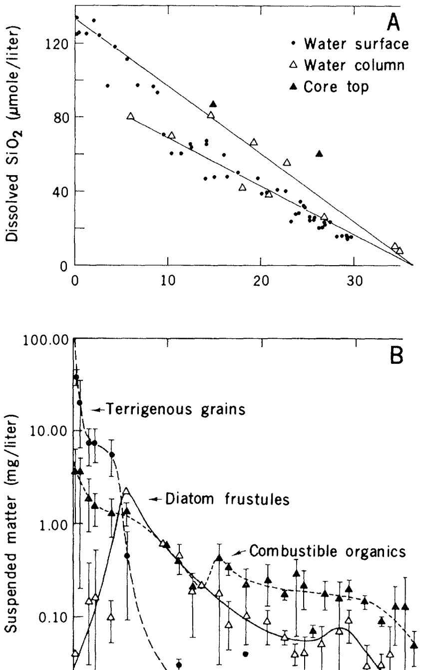

Fig. 1 (left). Sampling stations and oceanographic conditions off the Amazon River during 10 to 18 June 1974. Dots indicate surface stations, at which samples for suspended matter determinations were taken and salinity observations were made. Silica measurements were made at approximately half these stations. Open triangles are hydrographic stations at which samples were taken in the water column. River samples were taken at Belém and at Macapá in early June by E.B. Isopleths show the general trend of isohaline surfaces during the observation period. The cross-hatched area indicates where surface waters contained more than 20 mg of terrigenous grains per liter and the hatched areas indicate where they contained less than 0.06 mg/liter. Fig. 2 (right). (A) Dissolved silica plotted against salinity in surface waters, in the water column, and in core top waters on the Amazon shelf. The upper line describes an ideal mixing curve between Amazon River water on the left and ocean water on the right. The lower line indicates the inferred mixing line after biological uptake of silica. (B) Concentrations of terrigenous grains, diatom frustules, and combustible organic matter suspended within the surface waters off the Amazon River. These values represent averages, with the standard deviations also shown.

ported northward by longshore currents (*13*) or landward by currents within the tidal wedge (*15, 16*). It is difficult to estimate the quantity of frustules deposited along the northern coast since they are effectively masked by the large terrigenous load accumulating in these nearshore areas (*13*). However, a large portion of the frustules apparently is transported landward into the estuary: marine diatoms are common in the lower reaches of the Amazon River (*15*), and banks and bars off Marajo Island contain prominent dunes and interbedded layers of diatomite (*17*). If similar processes occur in other major estuaries, the actual amount of dissolved silica reaching the ocean may be considerably less than previously estimated.

JOHN D. MILLIMAN*
Woods Hole Oceanographic Institution, Woods Hole, Massachusetts 02543
EDWARD BOYLE
Woods Hole Oceanographic Institution and *Department of Earth and Planetary Sciences, Massachusetts Institute of Technology, Cambridge 02139*

References and Notes

1. P. S. Liss and M. J. Pointon, *Geochim. Cosmochim. Acta* **37**, 1493 (1973).
2. K. A. Fanning and M. E. Q. Pilson, *ibid.*, p. 2405.
3. E. Boyle, R. Collier, A. T. Dengler, J. M. Edmond, A. C. Ng, R. F. Stallard, *ibid.* **38**, 1719 (1974).
4. L. G. Sillen, in *Oceanography*, M. Sears, Ed. (AAAS, Washington, D.C., 1961), p. 549; F. T. MacKenzie and R. M. Garrels, *Science* **155**, 1404 (1966).
5. G. S. Bien, D. E. Contois, W. H. Thomas [*Geochim. Cosmochim. Acta* **14**, 35 (1958)] reported chemical removal of silica in the Mississippi River estuary, but "removal" probably was by dilution with low-silica waters from the open Gulf of Mexico and the shelf (*2, 3*).
6. Biological uptake of silica reported in the Scheldt estuary [R. Wollast and F. de Broeu, *Geochim. Cosmochim. Acta* **35**, 613 (1971)] may have actually been dilution by silica-poor coastal waters (*3*). More recently, silica uptake by diatoms in San Francisco Bay has been reported [T. J. Conomos and D. H. Peterson, *Mem. Inst. Geol. Bassin Aquitaine* 7, 45 (1974)].
7. J. D. Milliman, C. P. Summerhayes, H. T. Barretto, *J. Sediment. Petrol.* **45**, 189 (1975).
8. D. A. Livingstone, *U.S. Geol. Surv. Prof. Pap. 440-G* (1963); A. P. Lisitzin, *Soc. Econ. Paleontol. Mineral Spec. Publ. 17* (1972); R. E. Oltman, *U.S. Geol. Surv. Circ. 552* (1968).
9. Surface water samples were collected with plastic buckets and through tubing attached to a towed weight. Salinities were measured with an optical refractometer, accuracies being ± 0.3 per mil. Dissolved silica measurements were made by the method [illegible] J. D. Mullin and J. P. Riley [*Anal. Chim. Acta* **12**, 162 (1955)], using a salt correction factor, to an estimated precision of ± 3 percent. The scatter in the data plotted against salinity (Fig. 2A) is partly related to real variations within the estuary. Suspended matter samples were obtained by filtering seawater through paired, preweighed Millipore filters having nominal openings of 0.45 μm. Total and combustible concentrations were determined by standard methods [F. T. Manheim, R. H. Meade, G. C. Bond, *Science* **167**, 371 (1970)]. A portion of each filter was mounted on a glass slide and the quantity of terrigenous and noncombustible matter was estimated optically.
10. The Brazilian Directoria de Hidrografia e Navegação (personal communication) also reports two distinct areas of shoaling, just seaward of the Amazon River mouth and on the innermost shelf.
11. The rapid deposition of fine-grained particles at salinities lower than 3 per mil agrees with salt-flocculation experiments [for example, see U. G. Whitehouse, L. M. Jeffrey, J. D. Debbrecht, in *Proceedings of the 7th Conference on Clays and Clay Minerals*, A. Swineford, Ed. (Pergamon, New York, 1960), vol. 1] but available field data are inconclusive as to whether salt flocculation or organic agglomeration controls estuarine deposition of fluvial suspended sediments [R. H. Meade, *Geol. Soc. Am. Mem. 133* (1972), p. 91].
12. The paucity of samples precludes accurate calculation of diatom concentrations between 4 and 8 per mil, although in February 1973 diatom populations reached 4.5 mg/liter at 6 per mil (*7*).
13. L. A. Barreto, J. D. Milliman, C. A. B. Amaral, O. Francisconi, *Contrib. Sedimentol.* **4**, 11 (1975); J. D. Milliman, C. P. Summerhayes, H. T. Barretto, *Bull. Geol. Soc. Am.* **86**, 610 (1975).
14. Subsurface water samples coinciding with the upper curve contained few diatoms (0.01 to 0.03 mg/liter), suggesting low biological uptake of silica.

[illegible] F. Gessner and R. Simonsen, *Limnol. Oceanogr.* **12**, 709 (1967).

16. R. J. Gibbs, *J. Mar. Res.* **28**, 113 (1970).
17. W. A. Egler and H. O. Schwassmann, *Verh. Int. Ver. Limnol.* **15**, 1059 (1964).

18. Contribution No. 3505 of the Woods Hole Oceanographic Institution. Supported by International Decade of Ocean Exploration (IDOE) grant GX-41960, the National Science Foundation, and the Office of Naval Research (to J. M. Edmond). We thank L. Toner, C. Offinger, and L. Jablonski for help with collection and analysis of the samples, and J. M. Edmond, F. L. Sayles, and R. H. Meade for suggestions on the manuscript.

* Present address: Geological Survey of Canada, 100 West Pender, Vancouver B.C., Canada.

25 March 1975

Skeletal Low-Magnesium Calcite in Living Scleractinian Corals

Abstract. *The skeletons of living specimens of the scleractinian coral* Porites lobata *have been found to contain up to 46 ± 5 percent low-magnesium calcite even though free of gross detrital inclusions and boring or encrusting organisms. The calcite crystals occur in the interior of skeletal structures, have dimensions of 20 micrometers or less, and are surrounded by typical aragonite needles. Biogenic deposition seems to be the most likely source of the calcite, although the evidence does not rule out diagenesis of metastable aragonite on a time scale of months.*

The mineralogy and elemental composition of carbonate skeletons deposited by scleractinian corals have been examined by many workers (*1, 2*). Aragonite has been the only primary skeletal mineral thus far reported.

The diagenesis of metastable aragonite to low-magnesium calcite has also received much attention (*2, 3*). The results of these investigations show that under normal conditions in seawater the recrystallization is extremely slow, and skeletal aragonites of Pleistocene and older ages are not uncommon. We report here the discovery of skeletal low-magnesium calcite in living scleractinian corals.

Table 1. Age, percentage of calcite, and magnesium/calcium ratio in samples from two coral specimens (see Figs. 1 and 2); NA, no analysis.

Sample	Estimated age (years)	Mg/Ca atom ratio ($\times 10^3$) (± 8%)	Percentage of calcite (± 5%)
C1-1	0.3	NA	20
C1-2	0.7	4.3	17
C1-3	1.2	4.8	18
C1-4	1.8	4.2	22
C1-5	2.2	5.0	22
C1-6	2.8	5.1	27
C1-7	3.2	5.5	35
C1-8	3.8	5.5	39
C1-9	4.3	6.2	23
C1-10	4.8	6.2	46
C1-11	5.2	5.6	37
C1-12	5.8	4.8	26
C1-13	6.1	4.5	26
C1-14	6.3	3.6	6
C3-1	1.6	*	33
C3-2	4.8	*	26
C3-3	6.3	*	3
C3-4	?	†	4

*Calcite fraction Mg/Ca, $< 4 \times 10^{-2}$; no bulk analysis. †Calcite fraction Mg/Ca, 16×10^{-2}; no bulk analysis.

The primary study specimens were colonies of *Porites lobata* collected live from Waikiki reef off leeward Oahu, approximately 300 m offshore in 3 to 4 m of water. A variety of other archive specimens collected from various locations in the Pacific over the past 3 years were also surveyed.

X-radiography of slabs cut parallel to the axis of growth showed the usual seasonal density bands (*4*). Samples were taken from known locations in the alternating high- and low-density growth bands, from which the time of deposition of the carbonate could be estimated (see Fig. 1).

We carried out x-ray diffraction studies with an x-ray diffractometer (Norelco), using copper Kα radiation. All major aragonite and calcite peaks with *d*-values between 1.54 and 4.44 Å were identified. Samples were prepared, ground, and mounted by a variety of techniques (*5*), and control samples of known mineralogy were included in the study in order to eliminate the possibility of procedural artifacts. We calculated the percentage composition using the aragonite peaks with *d*-values of 3.27 and 3.40 Å and the calcite peak with a *d*-value of 3.03 Å. The calculated percentages agree with published calibrations (*6*).

Elemental analysis for strontium, calcium, and magnesium was carried out with an atomic absorption spectrophotometer (Perkin-Elmer model 303). In addition, the magnesium concentration in the calcite phase was estimated from the shift in the *d*-value of calcite parallel to its major cleavage (*7*).

Fresh, untreated fracture surfaces of the